

We are IntechOpen, the world's leading publisher of Open Access books Built by scientists, for scientists

6,900

Open access books available

186,000

International authors and editors

200M

Downloads

Our authors are among the

154

Countries delivered to

TOP 1%

most cited scientists

12.2%

Contributors from top 500 universities



WEB OF SCIENCE™

Selection of our books indexed in the Book Citation Index
in Web of Science™ Core Collection (BKCI)

Interested in publishing with us?
Contact book.department@intechopen.com

Numbers displayed above are based on latest data collected.
For more information visit www.intechopen.com



Prediction of Magnetite Segregation and Coal Partitioning In Dense Medium Cyclone Using Computational Fluid Dynamics Technique

M. Narasimha¹, M. S. Brennan², P.N. Holtham² and P.K. Banerjee¹

¹R&D Division, TATA Steel, Jamshedpur, Jharkhand 831 007,

²Julius Kruttschnitt Mineral Research Centre, The University of Queensland, Isles Road, Indooroopilly 4068, Queensland,

¹India

²Australia

1. Introduction

Dense medium cyclones are designed to partition coal particles based on particle density with the cut density adjusted by adding a finely dispersed heavy medium to the feed and adjusting the feed medium concentration. In a typical DMC, illustrated in Figure 1, a mixture of medium and raw coal enters tangentially near the top of the cylindrical section, thus forming a strong swirling flow. The denser high ash particles move along the wall of of

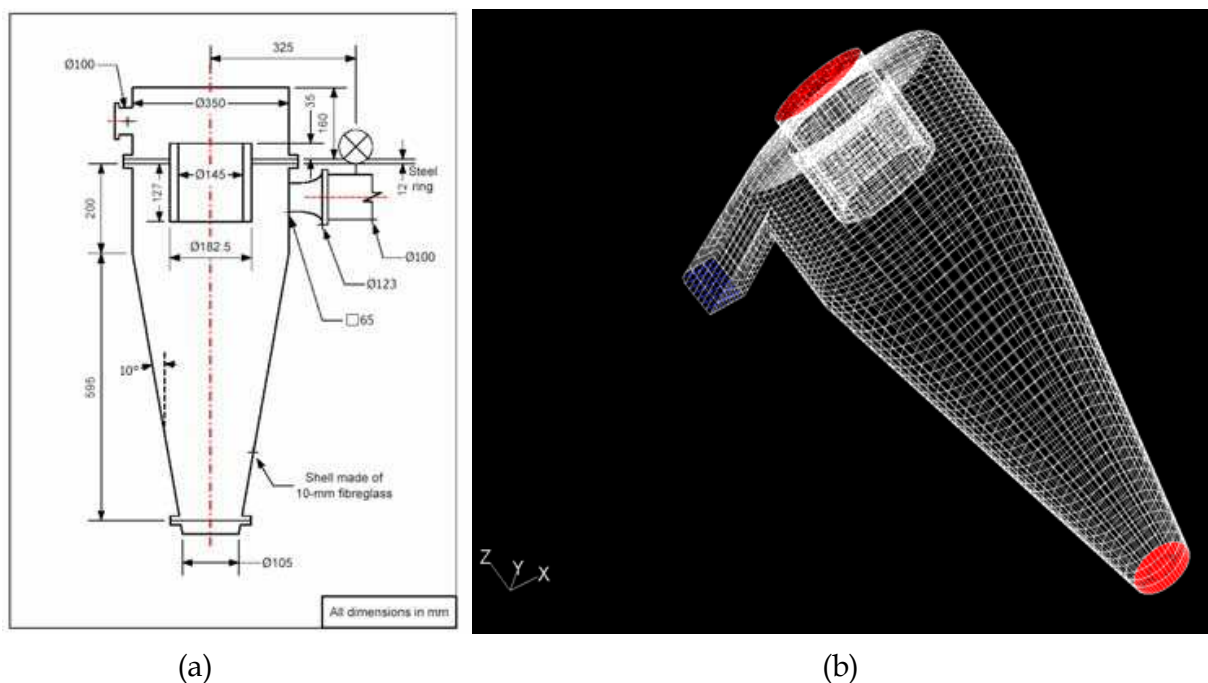


Fig. 1. (a) Detailed dimensional drawing of the 350 mm DSM dense medium cyclone used for simulations, (b) Grid generated in Gambit.

Source: Computational Fluid Dynamics, Book edited by: Hyoung Woo OH, ISBN 978-953-7619-59-6, pp. 420, January 2010, INTECH, Croatia, downloaded from SCIYO.COM

the cyclone due to the centrifugal force, where the velocity is downward and is discharged through the underflow orifice or the spigot. The lighter low ash coal moves towards the longitudinal axis where a strong up flow exists and passes through the vortex finder to the overflow chamber.

The presence of medium, coal particles, swirl and the fact that DMCs operate in the turbulent regime makes the flow behavior complex and studying the hydrodynamics of DMCs using Computational Fluid Dynamics (CFD) is a valuable aid to understanding their behaviour.

Most of the CFD studies have been conducted for classifying hydrocyclones (Davidson, 1994; Hsieh, 1988; Slack et al 2000; Narasimha et al 2005 and Brennan, 2006). CFD studies of DMCs are more limited (Zughbi et al, 1991, Suasnabar (2000) and Brennan et al, 2003, Narasimha et al (2006)). DMCs and Classifying cyclones are similar geometrically and the CFD approach is the same with both. A key problem is the choice of turbulence model. The turbulence is too anisotropic to treat with a k- ϵ model and this has led some researchers to use the differential Reynolds stress turbulence model. However some recent studies (Slack et al, 2000; Delagadillo and Rajamani, 2005; Brennan, 2006) have shown that the LES technique gives better predictions of the velocities in cyclones and seems to do so on computationally practical grids.

In this paper, CFD studies of multiphase flow in 350mm and 100mm Dutch State Mine (DSM) dense medium cyclone are reported. The studies used FLUENT with 3d body fitted grid and used the mixture model to model medium segregation, with comparisons between Large Eddy Simulation (LES) and Differential Reynolds Stress Model (DRSM) turbulence models. Predictions are compared to measured concentrations by GRT (Gamma ray tomography) and overall simulated performance characteristics using Lagrangian particle tracking for particles were compared to experimental data.

2. Model description

2.1 Turbulence models

The basic CFD approach was the same as that used by Brennan (2003). The simulations used Fluent with 3d body fitted grids and an accurate geometric model of the 350mm DSM pattern dense medium cyclone used by Subramanian (2002) in his GRT studies. The dimensions of the cyclone are shown in Figure 1a and a view of the grid used in the simulations is shown in Figure 1b. The equations of motion were solved using the unsteady solver and represent a variable density slurry mixture:

$$\frac{\partial \rho_m}{\partial t} + \frac{\partial \rho_m u_{mi}}{\partial x_i} = 0 \quad (1)$$

$$\begin{aligned} \frac{\partial}{\partial t}(\rho_m u_{mi}) + \frac{\partial}{\partial x_j}(\rho_m u_{mi} u_{mj}) = \\ - \frac{\partial}{\partial x_i} p + \frac{\partial}{\partial x_j}(\tau_{\mu,ij} + \tau_{d,ij} + \tau_{t,ij}) + \rho_m g_i \end{aligned} \quad (2)$$

The RANS simulations were conducted using the Fluent implementation of the Launder et al (1975) DRSM model with the Launder linear pressure strain correlation and LES

simulations used the Fluent implementation of the Smagorinsky (1966) SGS model. In the DRSM simulations $\tau_{i,ij}$ in equation (2) denotes the Reynolds stresses, whilst in the LES simulations $\tau_{i,ij}$ denotes the sub grid scale stresses. $\tau_{d,ij}$ is the drift tensor and arises in equation (2) as part of the derivation of the Mixture model (Manninen et al 1996). The drift tensor accounts for the transport of momentum as the result of segregation of the dispersed phases and is an exact term:

$$\tau_{d,ij} = \sum_{p=1}^n \alpha_p \rho_p u_{pm,i} u_{pm,j} \quad (3)$$

All equations were discretized using the QUICK option except that Bounded central differencing was used for momentum with the LES. PRESTO was used for Pressure and SIMPLE was used for the pressure velocity coupling. The equations were solved with the unsteady solver with a time step which was typically 5.0×10^{-4} s for both the DRSM simulations and LES simulations. The LES used the Spectral Synthesiser option to approximate the feed turbulence.

2.2 Multiphase modeling – mixture model with lift forces

The medium was treated using the Mixture model (Manninen et al 1996), which solves the equations of motion for the slurry mixture and solves transport equations for the volume fraction for any additional phases p, which are assumed to be dispersed throughout a continuous fluid (water) phase c:

$$\frac{\partial}{\partial t} \alpha_p + \frac{\partial}{\partial x_i} (\alpha_p u_i) + \frac{\partial}{\partial x_i} (\alpha_p u_{pm,i}) = 0 \quad (4)$$

$$u_{pm,i} = u_{pi} - u_i$$

$u_{pm,i}$ is the drift velocity of the p relative to the mixture m. This is related to the slip velocity $u_{pc,i}$ which is the velocity of the p relative to the continuous water phase c by the formulation:

$$u_{pmi} = u_{pci} - \sum_{l=1}^n \frac{\alpha_l \rho_l}{\rho_m} u_{lci} \quad (5)$$

$$u_{pci} = u_{pi} - u_{ci}$$

Phase segregation is accounted for by the slip velocity which in Manninen et al's (1996) treatise is calculated algebraically by an equilibrium force balance and is implemented in Fluent in a simplified form. In this work Fluent has been used with the granular options and the Fluent formulation for the slip velocity has been modified where (i) a shear dependent lift force based on Saffman's (1965) expression and (ii) the gradient of granular pressure (as calculated by the granular options) have been added as additional forces. Adding the gradient of granular pressure as an additional force effectively models Bagnold dispersive forces (Bagnold 1954) and is an enhancement over our earlier work (Narasimha et al, 2006).

$$u_{pci} = \frac{d_p^2 (\rho_p - \rho_m) *}{18 f_{rep} \mu_c} \left(\begin{array}{l} g_i - \frac{\partial}{\partial t} u_{mi} - u_{mj} \frac{\partial}{\partial x_j} u_{mi} + \\ 0.75 \frac{\rho_c}{\rho_p - \rho_m} C_{lp} \varepsilon_{ijk} \omega_{mj} u_{pck} - \frac{1}{\alpha_p (\rho_p - \rho_m)} \frac{\partial}{\partial x_i} P_{pg} \end{array} \right) \quad (6)$$

Equation (6) has been implemented in Fluent as a custom slip velocity calculation using a user defined function. f_{rep} has been modelled with the Schiller Naumann (1935) drag law but with an additional correction for hindered settling based on the Richardson and Zaki (1954) correlation:

$$f_{rep} = (1 + 0.15 \text{Re}_p^{0.687}) \alpha_p^{-4.65} \quad (7)$$

The lift coefficient has been calculated as

$$C_{lp} = 4.1126 \left(\frac{\rho_f d_p^2 |\omega|}{\mu_c} \right) f_c \quad (8)$$

f_c corrects the lift coefficient using the correlation proposed by Mei (1992).

2.3 Medium rheology

The mixture viscosity in the region of the cyclone occupied by water and medium has been calculated using the granular options where the Gidaspow et al (1992) granular viscosity model was used. This viscosity model is similar to the Ishii and Mishima (1984) viscosity model used in earlier work (Narasimha et al 2006) in that it forces the mixture viscosity to become infinite when the total volume fraction of the medium approaches 0.62 which is approximately the packing density and has the effect of limiting the total medium concentration to less than this value. However the Gidaspow et al model (1992) also makes the viscosity shear dependant.

2.4 Medium with size distribution

The mixture model was set up with 8 phase transport equations, where 7 of the equations were for medium which was magnetite with a particle density of 4950 kg.m⁻³ and 7 particle sizes which were; 2.4, 7.4, 15.4, 23.8, 32.2, 54.1 and 82.2 μm . The seventh phase was air, however the slip velocity calculation was disabled for the air phase thus effectively treating the air with the VOF model (Hirt & Nichols 1981). The volume fraction of each modeled size of medium in the feed boundary condition was set so that the cumulative size distribution matched the cumulative size distribution of the medium used by Subramanian (2002) and the total feed medium concentration matched Subramanian's (2002) experimental feed medium concentrations.

2.5 Coal particle tracking model

In principle the mixture model can be used to model the coal particles as well as medium but the computational resources available for this work limited simulations using the

mixture model to around 9 phases, and it was impractical to model coal with more than two sizes or densities simultaneously with 6 medium sizes. Thus the Fluent discrete particle model (DPM) was used where particles of a known size and density were introduced at the feed port using a surface injection and the particle trajectory was integrated through the flow field of a multiphase simulation using medium. This approach is the same as that used by Suasnabar (2000).

Fluent's DPM model calculates the trajectory of each coal particle d by integrating the force balance on the particle, which is given by equation (10):

$$\frac{Du_{d,i}}{dt} = k_d(u_{m,i} - u_{d,i}) + g_i \left(\frac{\rho_d - \rho_m}{\rho_d} \right) \quad (9)$$

k_d is the fluid particle exchange coefficient:

$$k_d = \left(\frac{18\mu_m d_d^2}{\rho_d} \right) \left(\frac{C_D Re_d}{24} \right) \quad (10)$$

The presence of medium and the effects of medium segregation are incorporated in the DPM simulations because the DPM drag calculation employs the local mixture density and local mixture viscosity which are both functions of the local medium concentration. This intrinsically assumes that the influence of the medium on coal partitioning is a primarily continuum effect. i.e., the coal particles encounter (or "see") only a dense, high viscosity liquid during their trajectory. Further the DPM simulations intrinsically assume that the coal particles only encounter the mixture and not other coal particles and thus assume low coal particle loadings.

To minimize computation time the DPM simulations used the flow field predicted by the LES at a particular time. This is somewhat unrealistic and assumes one way coupling between the coal particles and the mixture.

3. Results

3.1 Velocity predictions

The predicted velocity field inside the DSM geometry is similar to velocities predicted in DMCs by Suasnabar (2000). Predicted flow velocities in a 100mm DSM body were compared with experimental data (Fanglu and Wenzhen (1987)) and shown in Fig 2(a) and 2(b). Predicted velocity profiles are in agreement with the experimental data of Fanglu and Wenzhen (1987), measured by laser doppler anemometry.

3.2 Air core predictions

Figure 3 shows a comparison between the air core radius predicted from LES and DRSM simulations and the air core measured by Subramanian (2002) by GRT in a 350mm DSM body. In particular Figure 3 shows that the air core position is predicted more accurately by the LES and that the radius predicted by the RSM is smaller than experimental measurements in the apex region. This is consistent with velocity predictions because a lower prediction of the tangential velocity (as predicted by the DRSM) should lead to a thicker slurry/water region for the same slurry/water feed flow rate and therefore a thinner air core. This lends some cautious credibility to the LES velocity predictions.

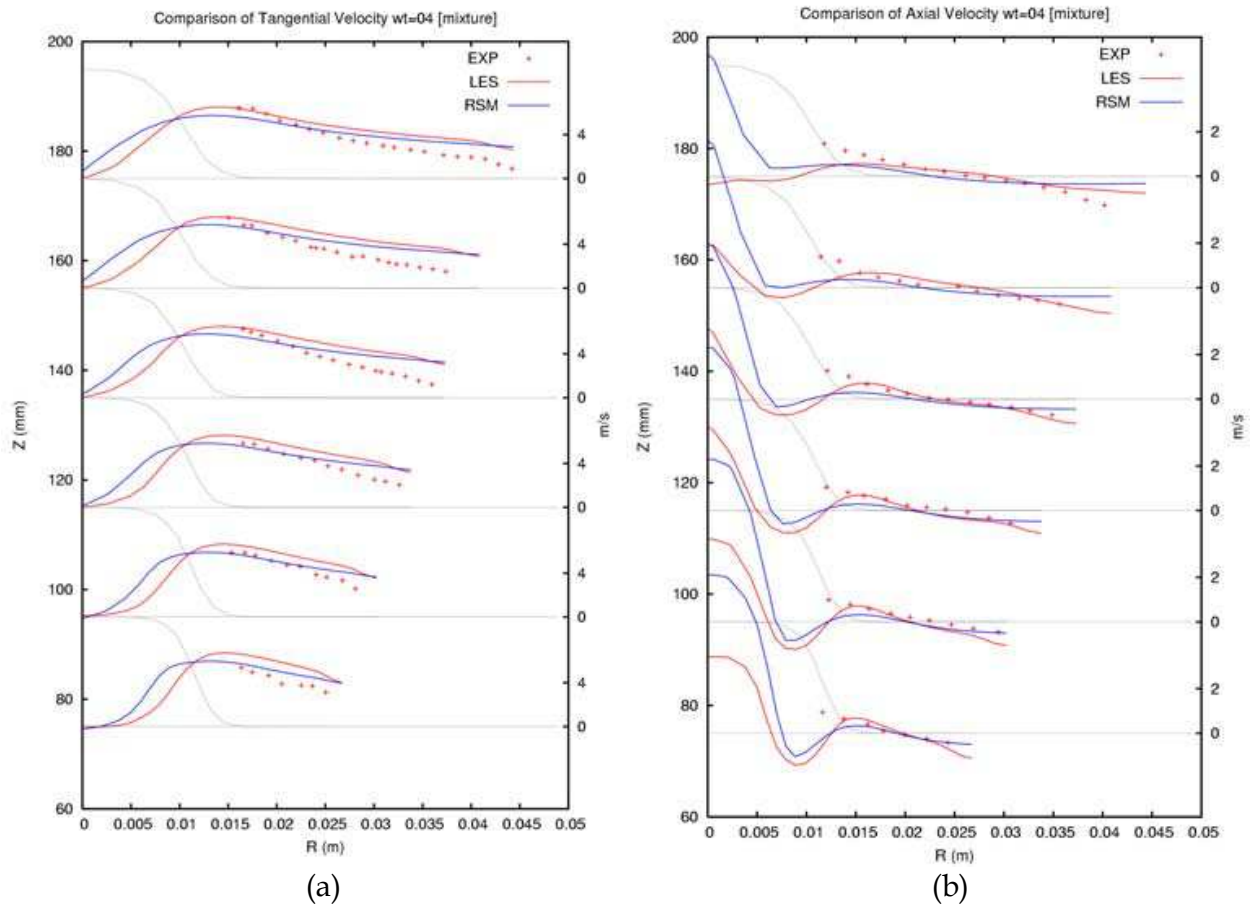


Fig. 2. Comparison of predicted (a) tangential velocity field, (b) axial velocity field with experimental data (Fanglu and Wenzhen (1987))

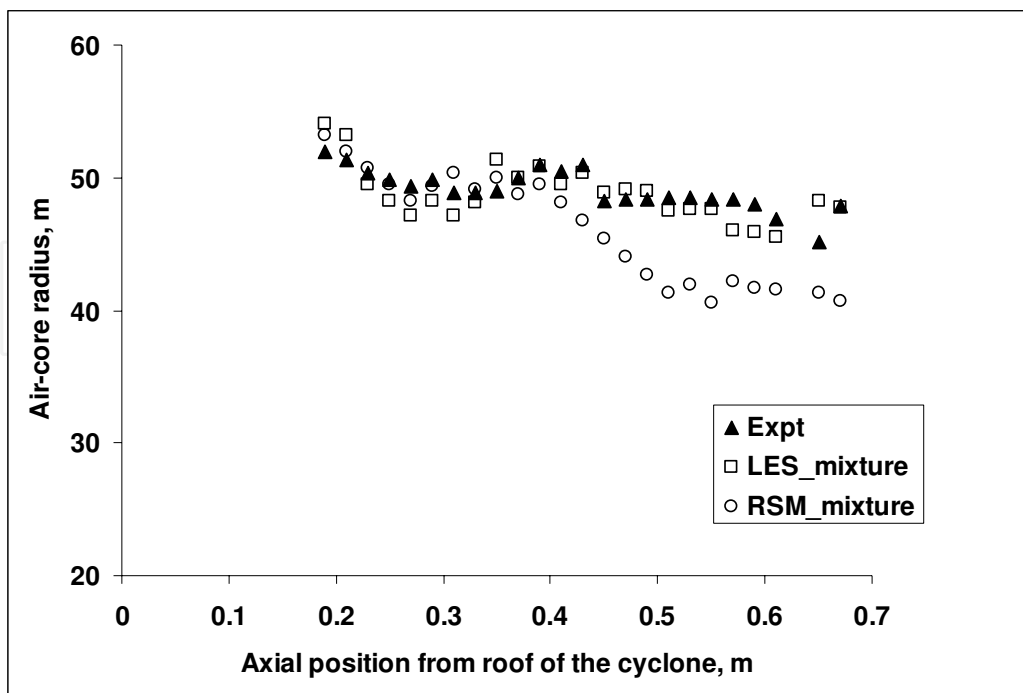


Fig. 3. Comparison between predicted and measured air core positions

3.3 Turbulence analysis of two phase flow in DSM body

Using the LES turbulence model, an analysis was made of the two phase (air-water) turbulence in a 350 mm DSM body. Figure 4 shows that in the DSM design, a very high turbulent kinetic energy occurs near the tip of vortex finder. As expected, the sudden transition from the cylindrical body to the conical section is a clear source of turbulent fluctuations down the cyclone body. These fluctuations propagate a very high turbulent kinetic energy near the bottom of the apex zone.

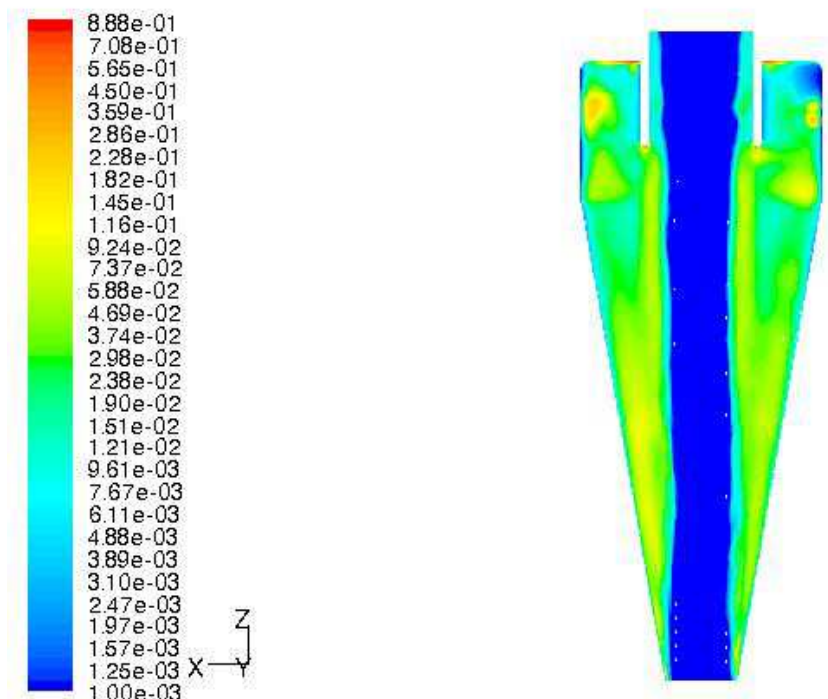


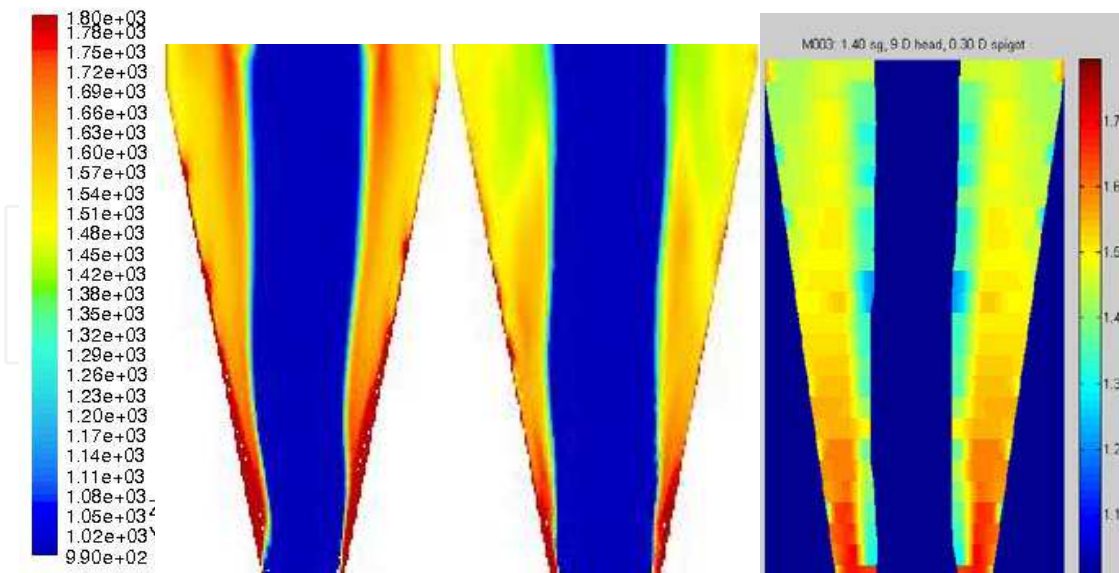
Fig. 4. Predicted turbulent kinetic energy contours in 350 mm DSM body

3.4 Prediction of medium segregation using medium feed size distribution, lift forces and viscosity corrections

Figure 5 shows the density profiles predicted by the CFD at steady flow for a feed RD of 1.465 and a feed head of 9Dc (equivalent to a volumetric flow rate of $0.0105 \text{ m}^3 \cdot \text{s}^{-1}$) together with an experimentally measured density profile for the same feed conditions from Subramanian (2002). Figure 5a shows the density profile using the modelling approach reported in Brennan (2003) and Brennan et al (2003) which is the basic mixture model with DRSM turbulence, Schiller Naumann drag relationship and a single medium size of $30 \mu\text{m}$, Figure 5b shows the density profile for the latest work which is from an LES using the mixture-granular model, medium with a feed size distribution, Schiller Naumann drag relationship with hindered settling, Lift and Bagnold forces and the Gidaspow et al (1992) granular viscosity law.

Figure 6 is a graphical comparison of the same data shown in Figure 5 at an elevation of 0.27 m and 0.67 m below the top of the cyclone body. 0.27m is the beginning of the apex and 0.67m is the lowest point at which Subramanian (2002) collected data. The predicted overflow and underflow medium densities are listed in Table 1.

The simulations from earlier work (Brennan 2003, Brennan et al 2003) with the basic mixture model, DRSM, single particle size, no lift and viscosity corrections display excessive



(a) DRSM-Brennan (2003) (b) LES latest work (c) GRT data- Subramanian (2002)

Fig. 5. Comparison between predicted slurry densities (a) DRSM-Mixture from Brennan (2003) (b) LES-Mixture latest work (see text left) (c) Experimental - Subramanian, 2002 for feed RD of 1.465, Feed head = $9D_c$ ($Q_f = 0.0105 \text{ m}^3 \cdot \text{s}^{-1}$); in elevation.

medium segregation although some of the characteristics of the distribution of medium are captured even though the predictions are inaccurate. At both 0.27m and 0.67m the medium concentration is excessive in the centre of the slurry region, and increases to a very large concentration at the wall at 0.67m.

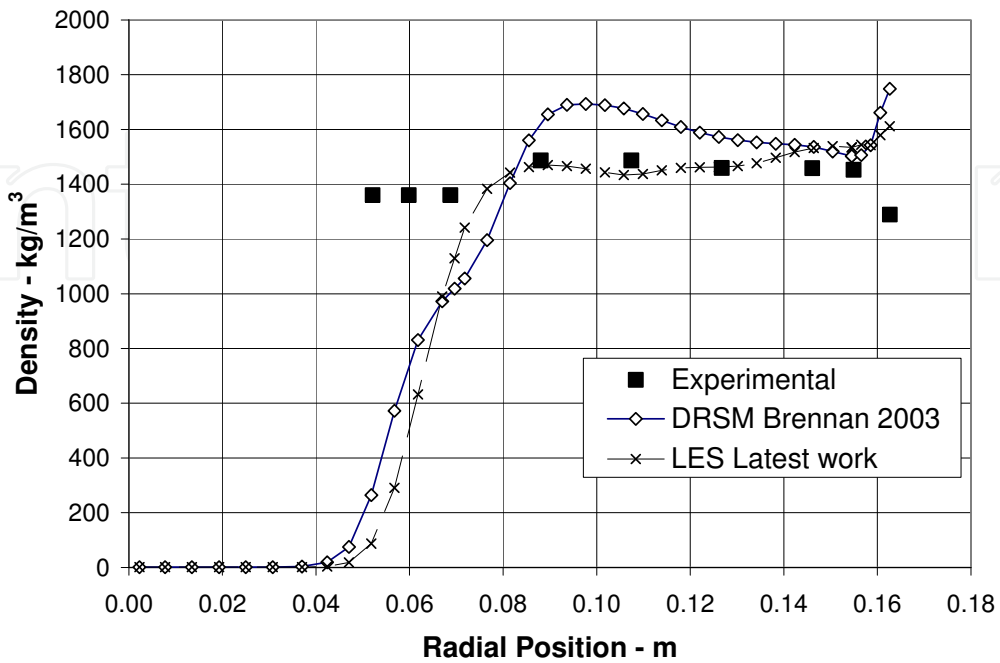
The LES with the mixture model enhancements is much more realistic. The improved accuracy however can be attributed to all of the enhancements. The medium used in Subramanian's (2002) GRT studies contained a significant distribution of sizes between 4 and $40 \mu\text{m}$ and one would expect that the smaller size would not segregate to the same degree as the larger size. Hence modeling the medium size distribution is necessary.

Finally the LES model is an enhancement over the DRSM turbulence model. This is partly because it is believed that it predicts the tangential velocities more accurately but also because LES resolves the larger scale turbulent fluctuations which generate turbulent mixing of the medium and this mixing is resolved because the instantaneous velocities are passed to the slip velocity calculation.

Turbulence model	Overflow, $\text{kg} \cdot \text{m}^{-3}$	Underflow, $\text{kg} \cdot \text{m}^{-3}$	Recovery to underflow
DRSM	1194	2232	0.256
LES	1339	1978	0.175
Experimental	1375	2076	0.137

Table 1. Predicted Flow densities and recovery to underflow - (a) DRSM-Mixture from Brennan (2003) (b) LES-Mixture latest work, (c) Experimental from Subramanian (2002) (feed RD of 1.465, Feed head = $9D_c$, $Q_f = 0.0105 \text{ m}^3 \cdot \text{s}^{-1}$)

Slurry Density at 0.27 m



Slurry Density at 0.67 m

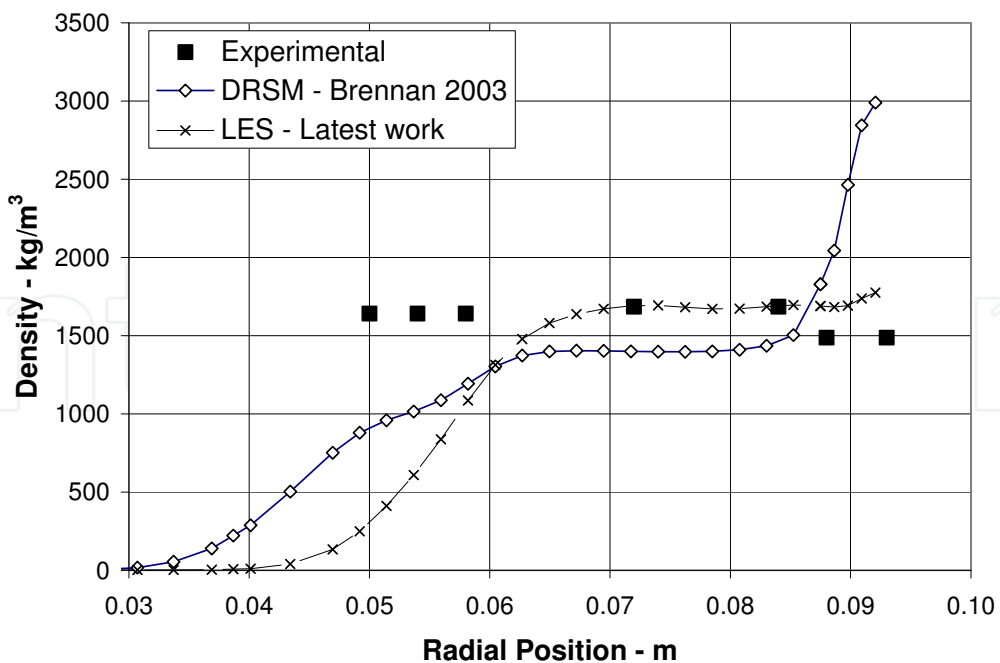


Fig. 6. Comparison between density contours predicted (LES and RSM models) by CFD and those measured by gamma ray tomography (a) at 0.27m, (b) 0.67m from roof of cyclone (Subramanian, 2002) for feed RD of 1.465.

3.5 Prediction of Magnetite segregation at different feed slurry densities

Medium segregation was studied with superfine magnetite at three feed solids concentrations (6.12, 7.5 and 11.62 % by volume), corresponding to medium densities of 1245, 1300 and 1465 kg m⁻³. Comparison of density contours between the measured densities of Subramanian (2002) and the medium densities predicted using the modified CFD multi-phase with LES turbulence modified mixture model are shown in Figure 7. The quantitative density comparisons are made in Table 2. The overflow and the underflow densities are predicted well by the LES multi-phase model. Table 2 also shows predictions from the Wood (1990) and Dungalson (1999) models which are empirical models based on a compendium of experimental data for the DSM geometry and these models are close to the experimental values.

Case		Dungalson DMC model	Wood DMC model	Experimental values	CFD predictions
M001	Feed density, kg.m ⁻³	1237	1237	1240	1237
	Under flow density, kg.m ⁻³	1844	1725	1834	1710
	Over flow density, kg.m ⁻³	1130	1114	1151	1144
	R _{uv} (under flow volumetric fraction)	0.15	0.143	0.1304	0.157
M002	Feed density kg.m ⁻³	1300	1300	1299	1300
	Under flow density, kg.m ⁻³	1930	1769	1889	1867
	Over flow density, kg.m ⁻³	1188	1182	1203	1189
	R _{uv} (under flow volumetric fraction)	0.151	0.143	0.143	0.162
M003	Feed density, kg.m ⁻³	1467	1467	1467	1467
	Under flow density, kg.m ⁻³	2073	1868	2076	1976
	Over flow density, kg.m ⁻³	1351	1366	1375	1339
	R _u (under flow volumetric fraction)	0.154	0.142	0.137	0.175

Table 2. Comparison of flow densities predicted by CFD (LES-Mixture model) with experimental densities and densities predicted by empirical models. Feed head = 9Dc

From Figure 7, it is observed that an increase in the medium feed concentration increases the density gradient across the radius of cyclone from the air core to the wall of the cyclone. Also the axial medium segregation increases; hence an increase in density differential is expected (see the Figure 8). This effect can be interrelated with changes of medium viscosity in the DMC (He & Laskowski, 1994; Wood, 1990). It is expected that an increase in the feed solids concentration increases the medium viscosity. This increase in slurry viscosity at higher feed medium densities increases the drag on solid particles, which has the effect of reducing the particle terminal velocity, giving the particles less time to settle. This results an increased flow resistance of solid particles and further accumulation of solids near the wall and also at the bottom of the cyclone.

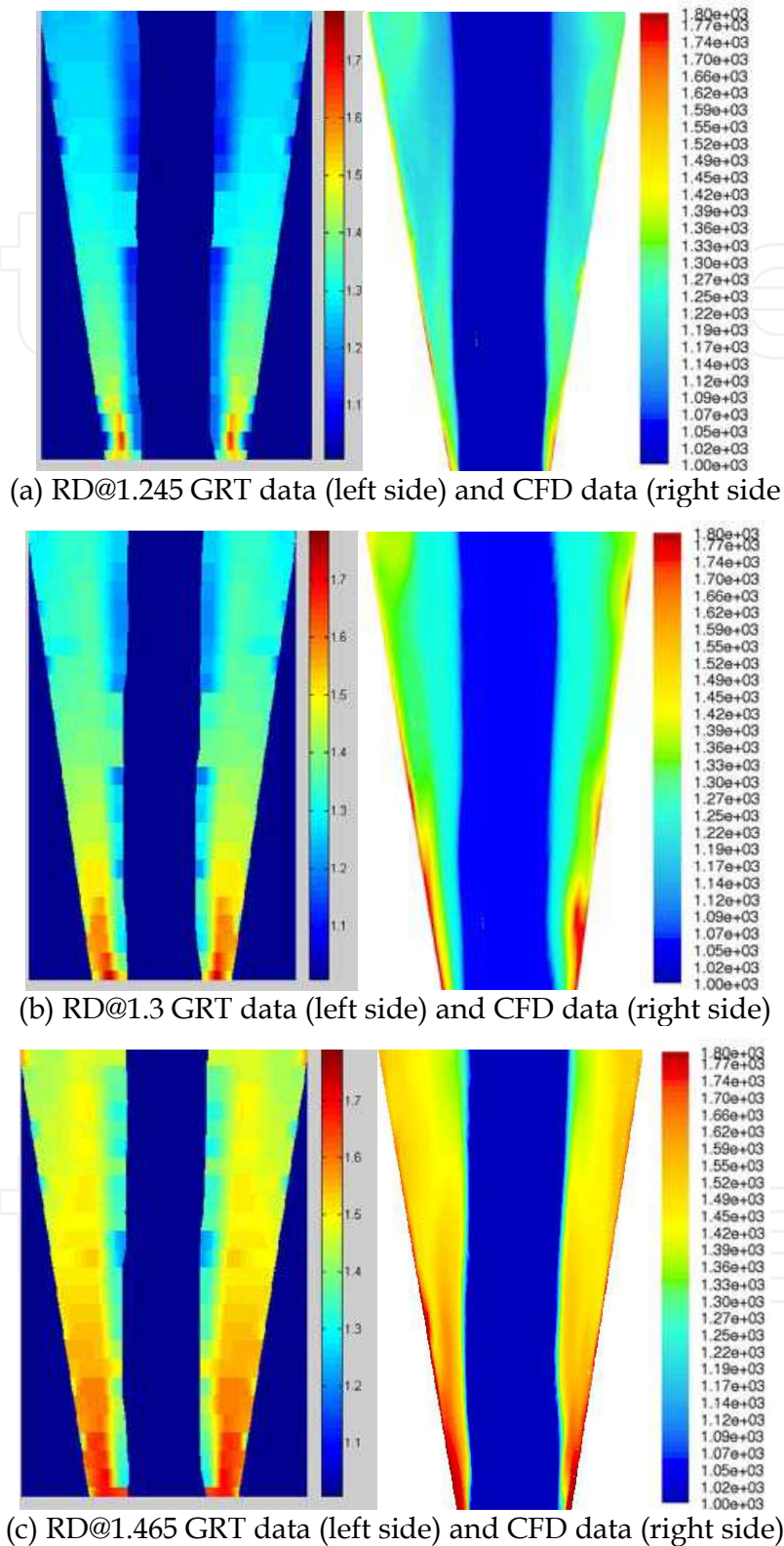


Fig. 7. Comparison between measured medium density contours (left side) by Subramanian (2002) and predicted medium density contours (right side) by CFD model at different feed medium relative densities (a) RD@1.245, (b) RD@1.3, and (c) RD@1.465 respectively.

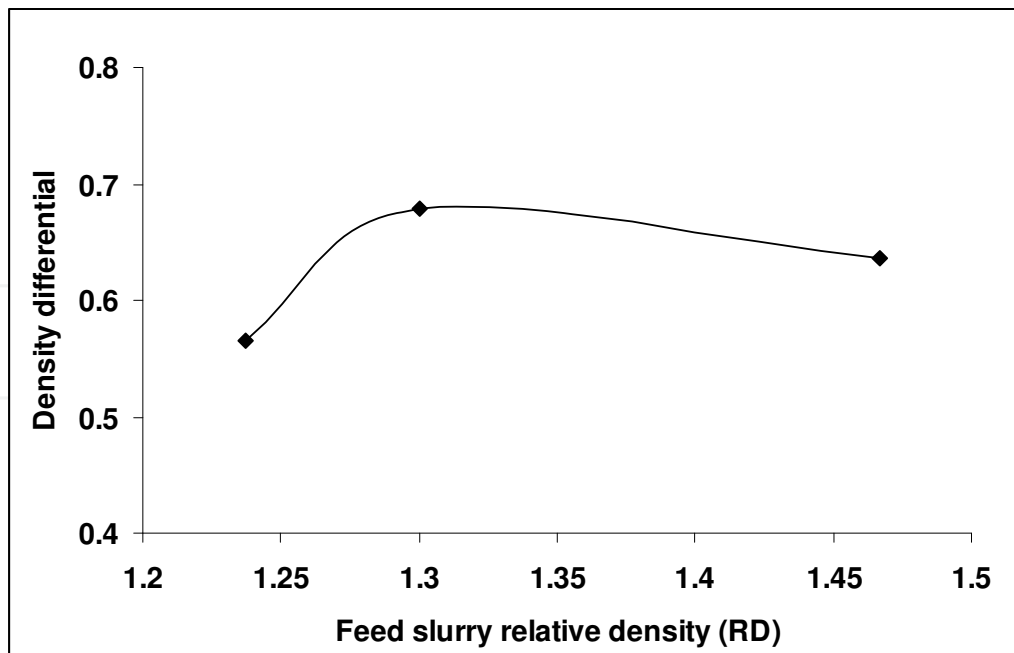


Fig. 8. Predicted density differential at various feed relative densities for superfine magnetite in DSM body

3.6 Effect of feed size distribution on medium segregation

The medium properties were modified by changing the particle size distribution. Effect of medium size distribution was investigated. Simulated sizes are given Table 3; the results are shown in Figure 9 and Table 4.

It was observed that reducing $d_{63.2}$ of medium reduces the segregation and density differential. Results are consistent with expected behaviour.

Magnetite sample	$d_{63.2}(\mu m)$	(Rosin-Rammler-Bennett constant) m
Fine	30.5	3.2
Superfine	20	1.6
ultrafine	17	1.45

Table 3. Particle size distribution of the tested magnetite samples

Magnetite	rho_u	rho_o	diff
Fine	2218	1267	951
Superfine	1987	1339	648
ultrafine	1949	1326	623

Table 4. Predicted density differential for a feed RD@1.465, at feed head = 9 Dc,

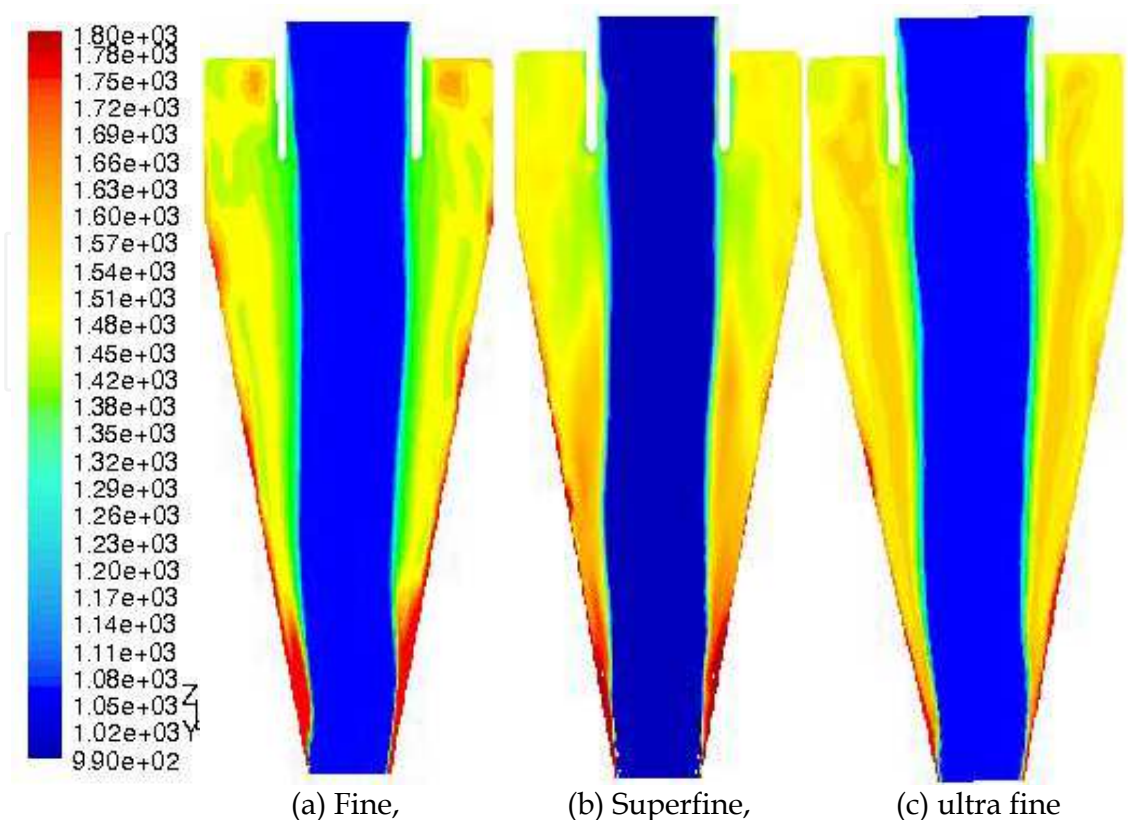


Fig. 9. Contours of medium density for (a) fine, (b) superfine and (c) ultrafine quality in DMC

3.7 Prediction of partition curve-pivot phenomena

Coal particles are typically in the range of 1100 and 1800 kg.m^{-3} in density and between 0.5 and 8 mm in size. DPM simulations were conducted where particles in this size range were injected at the feed and tracked. Each DPM simulation was repeated 5 times and 1050 particles were injected per simulation. The outlet stream to which each particle departed was noted and the information used to construct partition curves as function of particle density for given particle sizes. Figure 10 shows the partition curves so generated using a multiphase simulation with a feed RD of 1.2 and a feed head of $9D_c$.

As shown in figure 10, for the first time, the pivot phenomenon, in which partition curves for different sizes of coal pass through a common pivot point, has been successfully modelled using CFD. The predicted pivot parameters deviate slightly from the experimental data. The underflow split ratio and feed RD should be 14% and 1.236 from experimental observations whereas the CFD pivot point represents about 12% underflow flow ratio and pivot point relative density of 1.215 .

This comprehensive CFD model of dense medium cyclone is able to predict the performance of the DSM body reasonably well when compared to float-sink data of $-2 +0.5 \text{ mm}$ sized coal fraction (Hornsby and Wood 2000) (shown in figure 11). In particular, for the given set of design and operating condition, the predicted E_p value is about 0.075 , where as float and sink data represents about 0.0625 . The predicted E_p values are close to the experimental values although cut-point predictions deviate slightly. It is believed that the cut-point deviations are due to the interaction between coal particle-particles, which drive the extra resistance forces for the particle separation.

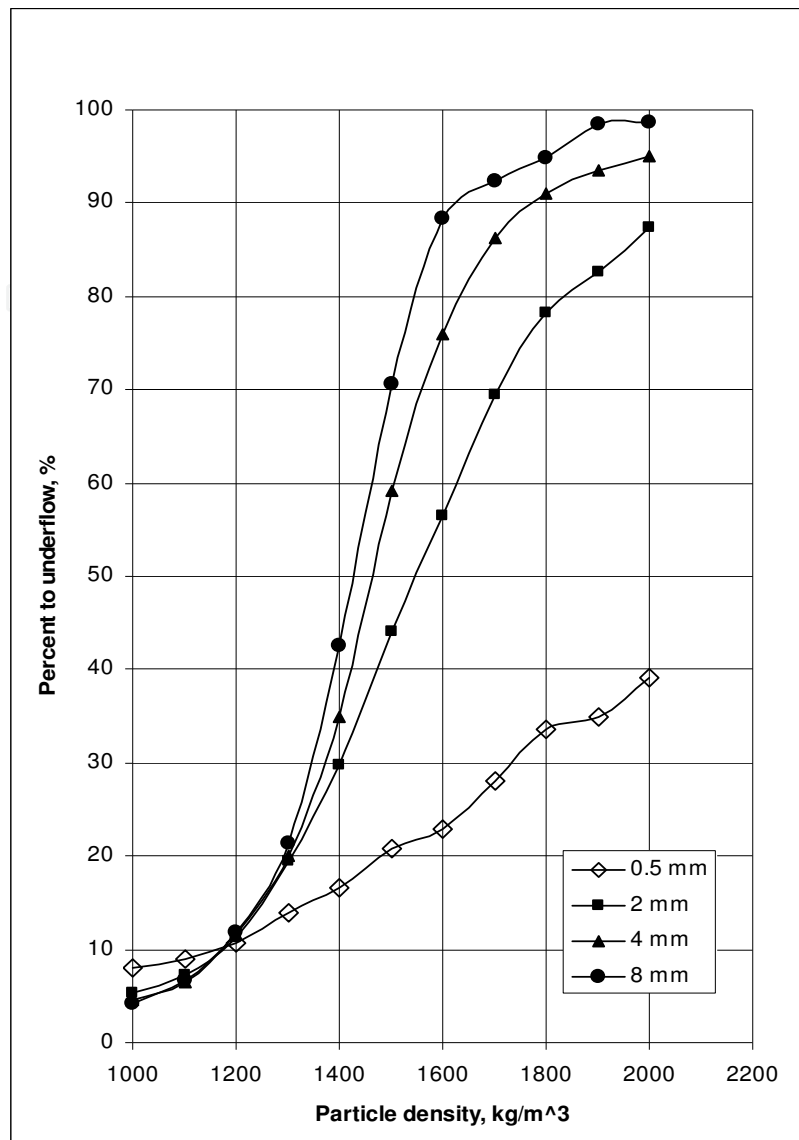


Fig. 10. Predicted size-by-size partition curves in a 350mm DSM cyclone

4. Conclusion

A large eddy simulation (LES) coupled with the Mixture Model has been applied to the study of medium segregation in a dense medium cyclone. The Mixture model was modified with corrections for wall lift forces, hindered settling, slurry rheology and particle interactions. Predicted velocity profiles are in agreement with the experimental data of Fanglu and Wenzhen (1987), measured by laser doppler anemometry. The multi-phase mixture model was modified with corrections for wall lift forces, hindered settling, and slurry rheology. Predicted density profiles are close to gamma ray tomography data (Subramanian (2002)) showing a density drop near the wall. At higher feed densities the agreement between the empirical correlations of Dungilson (1998), Wood (1990) and the CFD are reasonably good, but the overflow density from CFD is lower than the empirical model predictions and experimental values. The effect of size distribution of the magnetite has been fully studied. As expected, the ultra-fine magnetite sizes are distributed uniformly

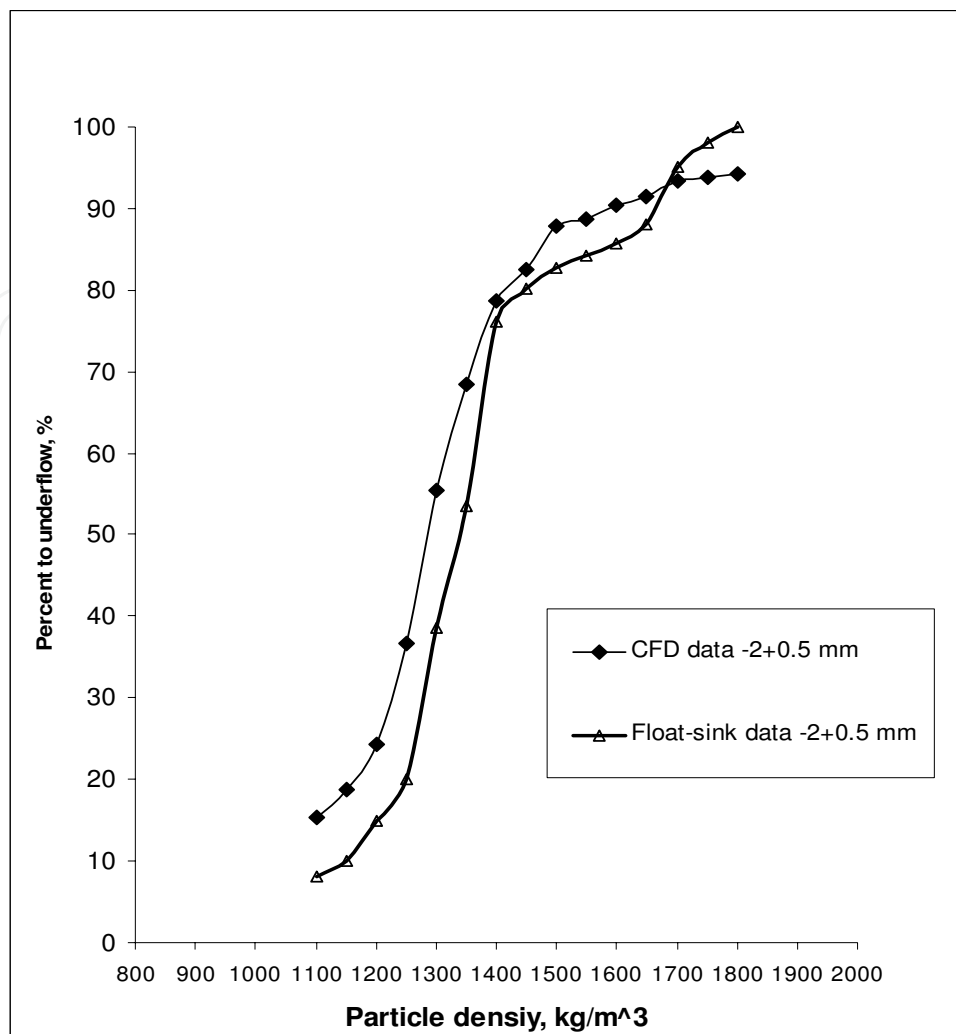


Fig. 11. Comparison of CFD prediction with float-sink data (Hornsby and Wood (2000), feed density RD =1.3 at 9Dc inlet head) in 350mm DSM.

throughout the cyclone. Once correct medium segregation was predicted, the performance characteristics of the DMC on coal were modelled using Lagrangian particle tracking for particles ranging in size from 0.5 to 8 mm. The predicted E_p values are very close to the experimental values although a slight deviation in the cut-point predictions was observed.

5. Acknowledgements

The authors would like to express their sincere thanks to Dr Debashish Bhattacharjee, Director RD&T, INDIA, TATA Steel groups and Prof. Tim Napier-Munn, Former Director of JKMRC, University of Queensland, Australia for their keen interest and encouragement for undertaking these studies.

NOMENCLATURE

Greek symbols

- α volume fraction
- ρ density kg.m⁻³

ε_{ijk}	permutation tensor
τ_{ij}	stress tensor $\text{kg.m}^{-1}.\text{s}^{-2}$
ω_{ij}	rotation or vorticity vector
μ	viscosity $\text{kg.m}^{-1}.\text{s}^{-1}$

Other symbols

C_d	drag coefficient
C_{lp}	lift coefficient
d	particle or phase diameter - m
D_c	cyclone diameter - m
E_p	cyclone efficiency parameter
f_{rep}	drag correction
F_{lpi}	lift force on particle - N
g_i	gravity - m.s^{-2}
k_d	fluid particle exchange coefficient
P_g	Granular pressure - pa
Re	Reynolds number
t	time - s
x_i	co-ordinate i - m
u_i	velocity - m.s^{-1}

Subscripts

c	continuous phase
d	discrete (coal) phase
m	mixture
p	particulate (medium) phase

6. References

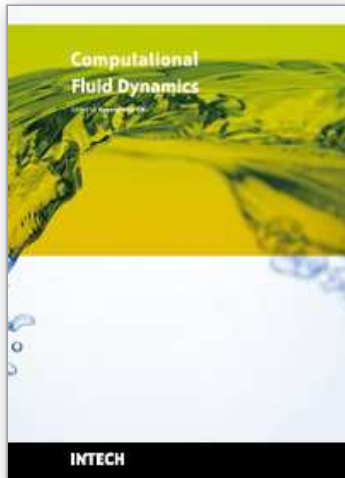
- BAGNOLD, R. A., (1954), "Experiments on a gravity free dispersion of large particles in a Newtonian fluid under shear", *Proc. Roy. Soc. London*, A225, 59-63.
- BRENNAN, M. S., (2003), "Multiphase CFD simulations of dense medium and classifying hydrocyclones", Proceedings of the 3rd International Conference on CFD in the Minerals and Process Industries, CSIRO Melbourne Australia, 10-12 December 2003, 59-63.
- BRENNAN, M.S, SUBRAMANIAN, V.J., RONG, R., HOLTHAM, P.N., LYMAN, G.J., AND NAPIER-MUNN, T.J., (2003), "Towards a new understanding of the cyclone separator", *Proceedings of XXII International Mineral Processing Congress, 29 September - 3 October, 2003, Cape Town, South Africa.*
- BRENNAN, M., (2006), "CFD simulations of hydrocyclones with an air core - comparison between large eddy simulations and a second moment closure", *Chemical Engineering Research and Design*, 84A, 495-505
- DAVIDSON, M., R., (1994), "A numerical model of liquid-solid flow in a hydrocyclone with high solids fraction", *FED-Vol 185, Numerical Methods in Multiphase Flows, ASME*, 29-39.

- DELGADILLO J.A., AND RAJAMANI, R. K., (2005), "A comparative study of three turbulence-closure models for the hydrocyclone problem", *International Journal of Mineral Processing*, 77, 217-230.
- FANGLU, G. AND WENZHEN, L., (1987) "Measurement and Study of Velocity Field in Various Cyclones by Use of Laser Doppler Anemometry", *3rd International Conference on Hydrocyclones, Oxford, England, 30 September 1987*
- GIDASPOW D., BEZBURUAH R, DING J. (1992), "Hydrodynamics of Circulating Fluidized Beds, Kinetic Theory Approach. ", *In Fluidization VII, Proceedings of the 7th Engineering Foundation Conference on Fluidization*, pages 75-82
- HIRT, C. W., AND NICHOLS, B. D., (1981), "Volume of fluid (VOF) method for the dynamics of free boundaries", *Journal of Computational Physics*, 39, 201-225.
- HORNSBY D., WOOD J. C., (2000), "Long cylinder dense medium cyclones for high near-gravity separations", ACARP project-C3010 report.
- HSIEH, K. T., (1988), "A phenomenological model of the hydrocyclone", Ph D Thesis, University of Utah.
- ISHII, M., AND MISHIMA, K., (1984), "Two-fluid model and hydrodynamic constitutive relations", *Nuclear Engineering and design*, 82, 107-126.
- KELSALL, D. F., (1952), "A study of the motion in a hydraulic cyclone", *Transactions of the Institution of Chemical Engineers*, 30, 87-104.
- LAUNDER, B.E., REECE, G.J., RODI, W., (1975), "Progress in the development of a Reynolds-stress turbulence closure", *Journal of Fluid Mechanics*, 68, 537-566.
- MANNINEN, M., TAIVASSALO V., KALLIO S., (1996), "On the mixture model for multiphase flow", Valtion Teknillinen Tutkimuskeskus, Espoo, Finland.
- MEI, R., (1992), "An approximate expression for the shear lift force on a spherical particle at finite Reynolds number", *Int. J. Multiphase flow*, 18, 145-147.
- NAPIER-MUNN, T.J., (1990), "The effect of dense medium viscosity on separation efficiency", *Coal Preparation*, 8, 145-165.
- NARASIMHA, M., BRENNAN, M. S., HOLTHAM, P. N., (2006), "Numerical Simulation of magnetite segregation in a dense medium cyclone", *Minerals Engineering*, 19, 1034-1047.
- NARASIMHA, M., SRIPRIYA, R. AND BANERJEE, P.K., (2005), "CFD modeling of hydrocyclone-prediction of cut size", *International Journal of Mineral Processing*, 75(1-2),53-68
- RICHARDSON, J. R., ZAKI, W. N. (1954) Sedimentation and Fluidization: Part I. *Trans. Inst. Chem. Eng.*, 32:35-53
- SAFFMAN P. G., (1965), "The lift on a small sphere in a slow shear flow", *Journal of Fluid Mechanics*, 22, 385-400.
- SCHILLER, L., NAUMANN, Z., Z. (1935), *Ver. Deutsch. Ing.*, 77, 318.
- SLACK, M.D., PRASAD, R.O., BAKKER, A., BOYSAN, F., (2000), "Advances in cyclone modeling using unstructured grids", *Transactions of the Institution of Chemical Engineers, Chemical Engineering Research and Design*, 78(A), 1098-1104.
- SMAGORINSKY, J., (1963), "General circulation experiments with the primitive equations. I. the basic experiment", *Monthly Weather Review*, 91, 99-164.
- SUASNABAR, D.J., (2000), "Dense Medium Cyclone Performance, Enhancements via computational modeling of the physical process", PhD Thesis, University of New South Wales.

- SUBRAMANIAN, V.J., (2002), "*Measurement of medium segregation in the dense medium cyclone using gamma-ray tomography*", PhD Thesis, JKMRRC, University of Queensland.
- ZUGHBI, H. D.; SCHWARZ, M.P.; TURNER, W.J. AND HUTTON, W., (1991), "*Numerical and experimental investigations of wear in heavy medium cyclones*", *Minerals Engineering*, 4, No. 3/4, 245-262.

IntechOpen

IntechOpen



Computational Fluid Dynamics

Edited by Hyoung Woo Oh

ISBN 978-953-7619-59-6

Hard cover, 420 pages

Publisher InTech

Published online 01, January, 2010

Published in print edition January, 2010

This book is intended to serve as a reference text for advanced scientists and research engineers to solve a variety of fluid flow problems using computational fluid dynamics (CFD). Each chapter arises from a collection of research papers and discussions contributed by the practiced experts in the field of fluid mechanics. This material has encompassed a wide range of CFD applications concerning computational scheme, turbulence modeling and its simulation, multiphase flow modeling, unsteady-flow computation, and industrial applications of CFD.

How to reference

In order to correctly reference this scholarly work, feel free to copy and paste the following:

M. Narasimha, M. S. Brennan, P.N. Holtham and P.K. Banerjee (2010). Prediction of Magnetite Segregation and Coal Partitioning In Dense Medium Cyclone Using Computational Fluid Dynamics Technique, Computational Fluid Dynamics, Hyoung Woo Oh (Ed.), ISBN: 978-953-7619-59-6, InTech, Available from: <http://www.intechopen.com/books/computational-fluid-dynamics/prediction-of-magnetite-segregation-and-coal-partitioning-in-dense-medium-cyclone-using-computational>

INTECH

open science | open minds

InTech Europe

University Campus STeP Ri
Slavka Krautzeka 83/A
51000 Rijeka, Croatia
Phone: +385 (51) 770 447
Fax: +385 (51) 686 166
www.intechopen.com

InTech China

Unit 405, Office Block, Hotel Equatorial Shanghai
No.65, Yan An Road (West), Shanghai, 200040, China
中国上海市延安西路65号上海国际贵都大饭店办公楼405单元
Phone: +86-21-62489820
Fax: +86-21-62489821

© 2010 The Author(s). Licensee IntechOpen. This chapter is distributed under the terms of the [Creative Commons Attribution-NonCommercial-ShareAlike-3.0 License](#), which permits use, distribution and reproduction for non-commercial purposes, provided the original is properly cited and derivative works building on this content are distributed under the same license.

IntechOpen

IntechOpen